Seismology

Introduction

In this class we will be concerned with *active source seismology*, or *exploration seismolog*y using man made seismic sources, in contrast to *passive seismology* or *earthquake seismology* that uses earthquakes of all sizes as natural sources. Broadly speaking, exploration seismology can be divided into two subareas – *refraction seismology* and *reflection seismology*. In a classic seismic refraction study, the principal data is the time taken for seismic energy to arrive at a given receiver location. The first arriving energy is always a refraction, in fact a Primary-wave or P-wave refraction. The travel-time data are inverted to create a model of the subsurface velocity structure and this velocity model is then interpreted to infer structural or geologic information, Figure 0a. Today, the inversion of times for structure is often referred to as *seismic tomography.* The distinction between the two is not clear cut, but the name seismic tomography is often preferred when the travel times of later arrivals such as reflections are included in the inversion or travel times between a large number of sources and receivers are used. Classic refraction seismology tended to use a small number of sources.

Reflection seismology is more interested in locating interfaces in the subsurface, e.g. sedimentary layer boundaries and faults across which either seismic velocity or density increases abruptly. The change in seismic properties cause a small fraction of the seismic energy to be reflected back to the surface and these “echoes” are recorded on the seismograms. In contrast to refraction work, reflection analysis uses the individual seismic records or *seismograms* directly to construct an image of the subsurface structure that is akin to geologic map. Determining velocity is not the primary objective of reflection work. However, the construction of an accurate image of subsurface structure from reflection data often requires a velocity model be generated as part of the processing. If the processing is incomplete the result will be a *seismic section* that really is a *pseudo-section:* a picture that shows many of the structural relationships within the subsurface, but with features not mapped to their true subsurface locaiton.

Traditionally, the principal user of seismic data has been the petroleum industry in the search for oil and gas deposits. These deposits are located in sedimentary structures for which the reflection method is the most powerful and most frequently used technique. Since drilling wells are very expensive, the industry puts a great deal of effort into getting an accurate 3-D picture of the subsurface, Figure 0b. These days the majority of oil company surveys are large 3-D reflections which require areal coverage using a very large number of sources and receivers. Even a modest 3-D survey can produce over 100 million seismograms.

Today, seismic reflection and refraction techniques are being applied to an ever wider variety of problems. These include general scientific investigations of crustal structure, location of earthquake faults, construction site surveys, water table location, archaeological and paleontological surveys. Reflection processing techniques are also used in the analysis of ground penetrating radar surveys.

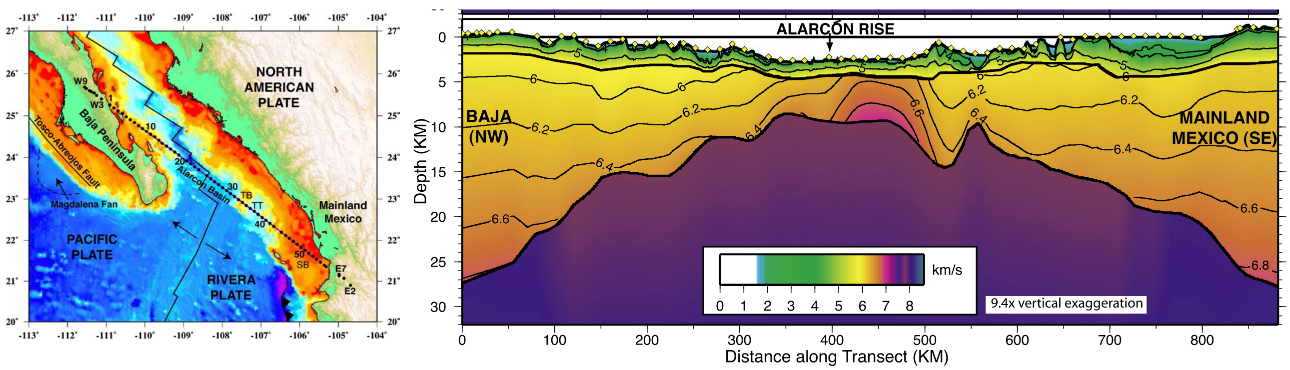

Figure 0a Example of a velocity model derived from a seismic refraction experiment. This is a model across the southern Gulf of California from Baja California to mainland Mexico. Roughly speaking green colors are velocity of 2-5 km/s. Orange colors correspond to velocities between 6-7 km/s and represent the lower crust, and dark blue colors are velocities above 8 km/s and represeent the mantle.

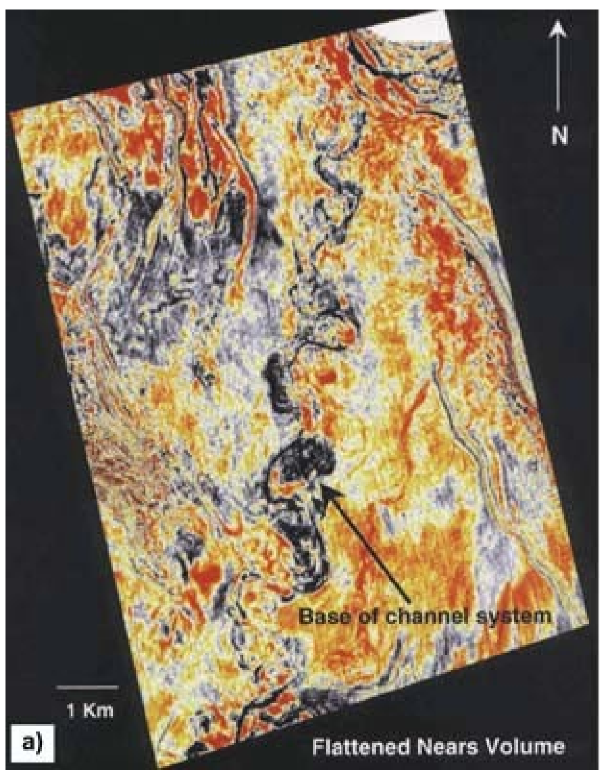

Figure 0b: A time slice, ~horizontal slice from a 3-D seismic reflection volume. Colors correspond to amplitudes of the processed seismic waves. The dark blue picks out the meandering path of an ancient buried offshore channel system from offshore Angola (Leading Edge, 20, Dec 2001.)

Revision

Basic properties of P-waves and S-waves.

Solid materials such as the earth support the propagation of two type of elastic waves, P-waves and S-waves. P-wave stands for *Primary wave*, because arrives first, and also for *comPressional wave*, because it propagates through a solid as series of compressions and dilatations; the motion of the solid, or *particle motion*, is parallel to the direction of wave propagation, Figure 1a. P-waves are sound waves in a fluid such as air or water. S-wave stands for *Secondary wave*, arriving after the P-wave, or *Shear wave*, as the direction of particle motion is perpendicular to the direction of wave propagation, Figure 5b. Thus unlike P-waves, the direction of S-wave particle motions is not completely determined by the propagation direction, and it is customary to consider a general S-wave to be the sum of *SH*, *shear horizontal*, and *SV, shear vertical*, components. The SH component as the name suggests has purely horizontal particle motions, but SV indicates only that the motion is confined to lie in a vertical plane containing the propagation direction, Figure 2.

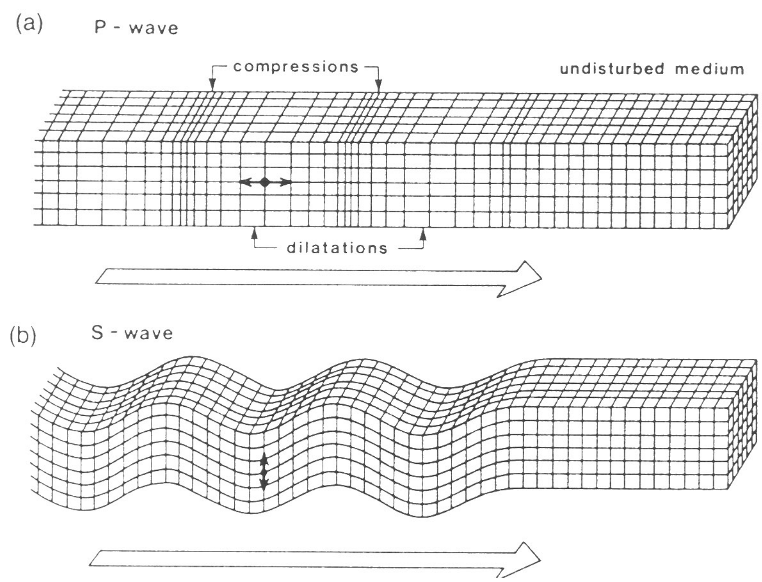

Figure 1: Elastic deformation and particle motions associated with the passage of body waves. (a) A P-wave. (b) An S-wave (after Bolt 1982.)

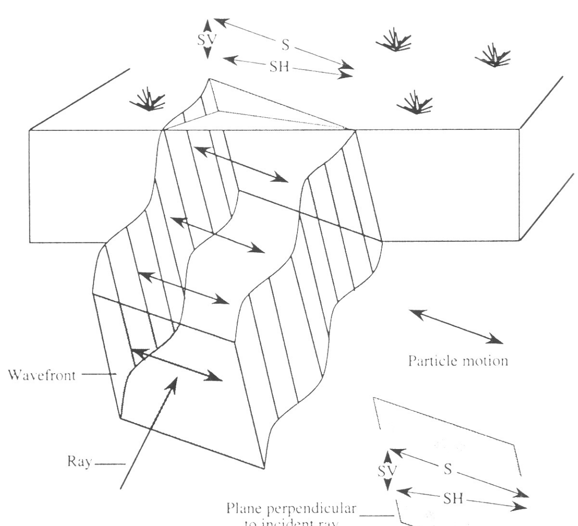

Figure 2: An S-wave incident at the ground surface. Since the wavefront plane containing the particle motions is at an angle to the horizontal , ground surface motion will have horizontal and vertical components. The motion can be resolved into an SH component parallel to the ground and an SV, vertical component.

The velocity of P-waves is denoted by α or v_p, while the velocity of S-wave is denoted by β or v_s. For a given material, v_p is always greater than v_s. Fluids only support P-waves, which is sometimes expressed by saying $v_s = 0$ for fluids. (We will assume throughout this course that the velocity of wave propagation is the same in all directions, that is, the materials of interest are isotropic. Wave propagation can vary with direction in which the underlying material is anisotropic. Anisotropy can be diagnostic of some important properties of the earth such as the predominant direction of cracking in an, or flow directions in the mantle but is beyond the scope of this course).

Body waves vs. Surface Waves

Until now, we have implicitly been talking about body waves; waves that are free to travel in any direction throughout the body of the earth. Another important class of seismic waves are surface waves, which is seismic energy trapped within the low velocity layers near the surface of the earth and traveling parallel to the earth's surface. There are 2 basic types of surface waves - *Rayleigh waves* and *Love waves*. Love waves, like SH waves, have particle motions which are perpendicular to the direction of propagation. Rayleigh waves are a combination P-SV waves and all their particle motion lies within a vertical plane containing the direction of propagation (see Figure 3). To exist, Love waves require velocity to increase with depth but the fundamental Rayleigh wave can exist even in a medium with uniform velocity provided it has a surface, a medium described as a *uniform half space*. The fundamental Rayleigh wave has retrograde elliptical particle motions whose amplitude decays exponentially with depth, and has a propagation velocity which is slightly less than the S-wave velocity. Other Rayleigh and Love waves have a more complicated amplitude variation with depth, but all decay exponentially below a certain depth. What constitutes a surface wave varies with scale and frequency of the seismic waves. In global seismology, surface waves can extend ~100 km and frequencies of 0.01 Hz, while for a hammer seismic experiment, the surface waves can be confined to the top 1 m or so of soil.

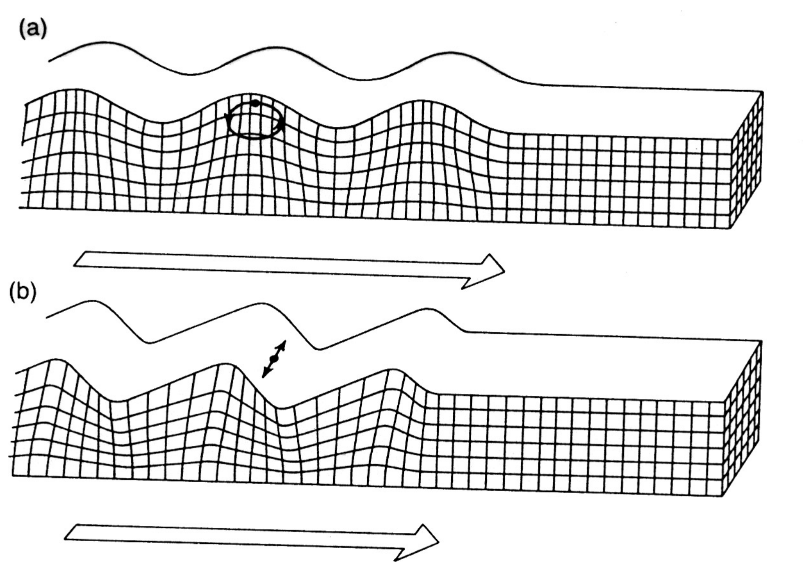

Figure 3 Surface Wave Displacements: (a) Rayleigh Wave. The particle motions of a fundamental Rayleigh wave are confined to the plane of propagation and are retrograde elliptical, that is the particle moves backwards at the top of its displacement. The amplitudes of the motions decay exponentially with depth. (b) Love wave. The particle motions are horizontal and perpendicular to the direction of propagation.

The Wave Equation

The 1-D wave equation

Let *u(x, t)* denote the displacement of a one-dimensional rod in the x-direction as a function of the undisturbed position *x* and time *t*, then 1-D wave equation describing the evolution of the disturbance with time is given by

$$\frac{\partial^2 u}{\partial x^2} = \frac{1}{v^2}\frac{\partial^2 u}{\partial t^2} \quad \text{where} \quad v^2 = K/\rho \qquad (1)$$

See accompanying text box for the derivation. Here v is the velocity of wave propagation, and is the ratio of the stiffness of the rod *K*, to the density ρ, which has dimension of the mass per unit length. The stiffness *K* relates the internal force within the rod, F, to the deformation as measured by the strain, the fractional increase in the length of a rod element, $\delta u/\delta x$ with original length δx

$$F = K\frac{\delta u}{\delta x}$$

This linear relationship between force and strain is an example of Hook'es Law. *K* is a measure of the resistance to deformation: the larger *K*, the more strongly the rod resists being stretched. Hooke's law is found to be a good approximation for most solids provided that the strains are small. *K* has dimensions of force, $[MLT^{-2}]$, while ρ has dimensions $[ML^{-1}]$ thus *v* has dimensions of velocity.

The 3-D scalar wave equation.

The derivation of the 1-D wave-equation can be generalized to three-dimensions, to derive the equation for acoustic waves in a fluid. Going from one to three dimensions adds second derivatives in all the space dimensions, and in terms of pressure fluctuations, p, the equation is

$$\nabla^2 p = \frac{1}{v^2}\frac{\partial^2 p}{\partial t^2} \qquad v = \sqrt{\frac{K}{\rho}} \qquad (2)$$

Here *v* is the velocity of compressional wave (P-wave) propagation in a fluids and is the ratio of the *bulk modulus*, *K,* to the density ρ. As before, this can be interpreted as the ratio of the restoring force to the inertia as represented by density. The bulk modulus measures the fluids resistance to compression, and appears in another expression of Hooke's law relating the fractional change in an elemental volume, *V*, to the change in the ambient pressure, *p*.

$$p = -K\frac{\Delta V}{V}$$

The sign is negative because an increase in the ambient pressure results in a decrease in the volume. Pressure is a measure of the force acting per unit area on surface either external or internal to the fluid, and is an example of a stress. Pressure always acts perpendicularly or normal to a surface and is for this reason termed a *normal stress*. It has units of $[ML^{-1}T^{-2}]$, while density has dimensions of $[ML^{-3}]$, thus *v* once again has dimensions of velocity.

Seismic Waves in a Solid

With a solid, forces can act in any direction on a surface, either internal or external. The force per unit area, or stress, can always be resolved into a normal stress and a tangential stress, known as a *shear stress*. It is the ability of the solid to support/resist shear stresses that distinguishes it from a fluid

Derivation of the 1-D Wave Equation

Let *u(x, t)* denote the displacement of the rod in the x-direction as a function of the undisturbed position *x* and time *t*. The wave equation is derived by considering the internal forces acting on a small element of the rod of length δ*x* between *x* and *x*+δ*x*.

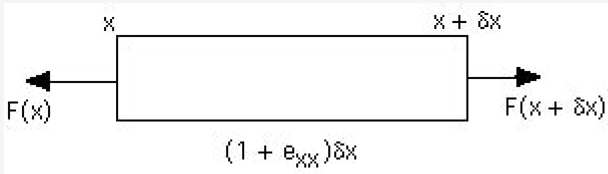

Describing rod deformation.

We cannot use the displacement *u(x)* directly as a measure of internal deformation of the rod, since if *u* is independent of *x*, the entire rod is simply translated without a change of shape. Instead, the strain, e_{xx}, defined as the fractional increase in the length of the rod element, is used.

$$e_{xx} = \frac{u(x+\delta x) - u(x)}{\delta x} = \frac{\partial u}{\partial x}$$

since $$u(x+\delta x) - u(x) \simeq \frac{\partial u}{\partial x}\delta x$$

Hooke's Law: the relationship between strain and the internal forces.

When the rod is deformed, internal forces will arise within the rod resisting deformation. The simplest assumption is that the rod obeys Hooke's law and that the internal force, *F*, is proportional to strain. Thus the force is given by

$$F = K\frac{\partial u}{\partial x} \qquad \text{(i)}$$

Hooke's law is found to be a good approximation for most solids provided that the strains are small. The constant of proportionality *K* has to be found empirically.

Balancing forces on a small element of the rod.

We can apply Newton's 2nd Law *F = ma* to a small rod element of undisturbed length δ*x*, which has mass ρ*dx*, if ρ is the mass per unit length of the rod. The force balance gives

$$F(x+\delta x) - F(x) = \rho\delta x\,\frac{\partial^2 u}{\partial t^2}$$

$$\frac{\partial F}{\partial x} = \rho\frac{\partial^2 u}{\partial t^2} \qquad \text{(ii)}$$

(If the acceleration is zero, the rod is in static equilibrium, with constant force, and, from (i), constant strain along the rod.) Substituting eqn (i) into eqn (ii) yields the one-dimensional wave equation.

$$\frac{\partial^2 u}{\partial x^2} = \frac{1}{v^2}\frac{\partial^2 u}{\partial t^2}$$ where $v^2 = K/\rho$

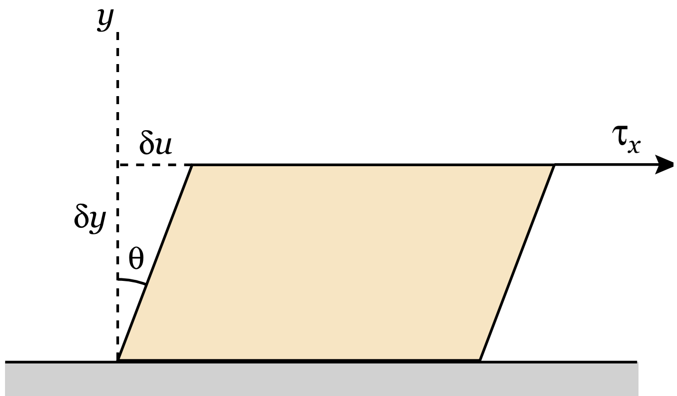

Figure 4 A shear stress, τ_x, applied to a block with a fixed base produces a displacement δu proportional to the height δu. This ratio is equal to shear angles, θ, for small angles, and $\tau_x = \mu\theta$

and permits the propagation of shear waves. The relevant modulus in this case is the shear modulus, μ. One expression for μ relates the shear stress in the x-direction, τ_x, to simple shear strain

$$\tau = \mu \frac{\partial u}{\partial y}$$

This can be visualized in terms of response of a small rectangular block, Figure 4.

The shear speed or S-wave speed of a solid is, once again the ratio of the restoring force to the density

$$\beta = v_s = \sqrt{\frac{\mu}{\rho}}$$

The shear strength of a solid modifies the compressional wave speed or P-wave speed to

$$\alpha = v_p = \sqrt{\frac{K + 4/3\mu}{\rho}} = \sqrt{\frac{\lambda + 2\mu}{\rho}}$$

The bulk modulus K and the shear modulus μ are both positive, so for a given solid the P-wave speed is always greater than the S-wave speed. λ and μ are known as the Lamé *parameters*. Unlike K and μ, λ has no simple physical interpretation but appears in the full mathematical description of the stress-strain relationship for solids.

Focus of Exploration Seismology

The primary focus of exploration seismology is on the use of reflected and refracted of P body waves.One reason for this focus is the relative ease with which P-waves can be generated with man-made sources. Explosives, for example, generate only P-waves, and all marine sources generate only P-waves since S-waves don't propagate in water. Analysis of surface wave plays a large role in earthquake seismology, but for the most part surface waves are considered to be noise exploration seismology, and in land exploration considerable effort can be expended trying to reduce their generation and recorded amplitude. This is not to say that either S-waves or surface waves have no role. The use of S-waves has increased significantly in recent years as both the sophistication of field techniques and analysis has improved.

For the most part P and S body waves can be thought of as propagating independently with each wave satisfying a 3-D scalar wave equation of the form (2) with the appropriate velocity. The condition for this separation to be valid is that velocities vary slowly. One place where this is not true is at interfaces between rocks, and significant energy conversion between two waves type can occur at interfaces. In the following, velocity will often be used without specifying vp or vs explicitly, in such cases, when in doubt, P-wave velocity should be assumed.

Factors Affecting Seismic Velocity

The accompanying table lists typical velocities for a variety of rock types. There is a range of velocities for any particular type of rock since seismic velocity is influenced by the precise mineral composition of the rock, the porosity and the pore fluid composition. Porosity and pore fluids can often be the dominant factors controlling velocity variations in the near surface and upper crust. Increased confining pressure tends to rapidly close cracks in less competent rock, while the change in pore fluid from, for example, air to water at the water table can produce a jump in velocity. Velocity is also influenced by the metamorphic history of a rock as increased depth of burial and heating tends to reduce porosity and encourage the formation of denser-faster minerals.

The factors affecting seismic velocity are for the most part the same factors affecting rock density and empirically a good correlation is found between density and compressional velocity, particularly for sedimentary rocks. The most well known of such relationships is the *Nafe-Drake curve*, see Figure 5. Thus density can be estimated from a knowledge of seismic velocity

There are similar empirical relationships between P-wave velocities and S-wave velocities. In general the ratio v_p/v_s lies in the range 1.7 -> 2.0.

Material	**Vp** (km/s)
Unconsolidate Materials	
Sand (dry)	0.2–1.0
Sand (water saturated)	1.5–2.0
Clay	1.0–2.5
Permafrost	3.5–4.0
Sedimentary Rocks	
Sandstones	2.0–6.0
Tertiary sandstone	2.0–2.5
Pennant Sandstone (Carboniferous)	4.0–4.5
Cambrian Quartzite	5.5–6.0
Limestones	2.0–60
Cretaceous chalk	2.0–2.5
Jurassic Oolites & bioclastic limestones	3.0–4.0
Carboniferous limestone	5.0–5.5
Dolomites	2.5–6.5
Salt	4.5–5.0
Igneous/Metamorphic rocks	
Granite	5.5–6.0
Gabbro	6.5–7.0
Ultramafics	7.5–8.5
Serpentinite	5.5–6.5
Pore Fluids	
Air	0.3
Water	1.4–1.5
Petroleum	1.3–14

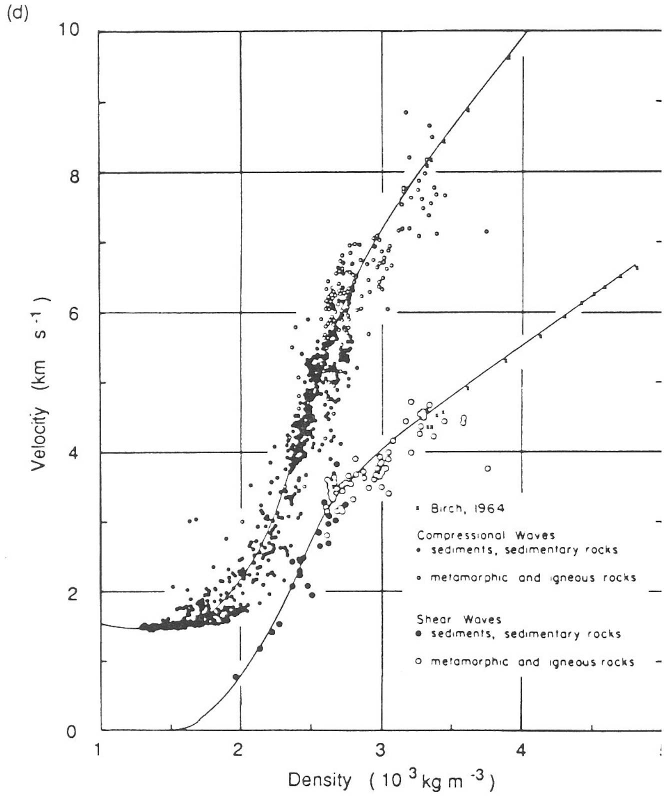

Figure 5: Nafe-Drake curve: The Nafe-Drake curve is an empirical relationship between seismic-velocity and density named after its originators. The curve spans the range of crustal & upper mantle values.

Solutions of the Wave Equation

We are not going pursue full solutions of the wave equation in detail but some simple solutions are useful for illustrating properties of seismic waves and seismograms such as amplitude and the connection to ideas such as *wavefronts* and *rays* that we will use in much or our analysis.

D'Alembert's solution to the 1-D wave equation

The general solution of the one-dimensional wave equation, (1), is known as *D'Alembert's solution* and is given by

$$u(x,t) = g(t-x/v) + h(t+x/v) \qquad (3)$$

The functions, g & h, are arbitrary and are determined by the initial conditions. We can verify that $u(x,t)$ is a solution of the 1-D wave equation by direct substitution in the wave equation (see text box). If we assume initially, for simplicity, that h = 0, and that we have a seismic source, $s(t)$ at $x = 0$.

then $u(0,t) = g(t) = s(t)$

so $\quad u(x,t) = s(t-x/v)$

Thus the arbitrary function in the general solution is determined by the seismic source. If the velocity $v = 2$, then at $x = 2$

$$u(2,t) = s(t-1)$$

The displacement at $x = 2$ is just the source function but delayed by 1 s (see Figure 6): the wave propagates without change of shape or amplitude. In general the arrival times of the wave are given by setting the argument of s to 0.

$$0 = t - x/v \qquad (4)$$

and the function $g(t-x/v)$ corresponds to a wave propagating in the positive x-direction. Similarly $h(t+x/v)$ represents a wave propagating in the negative x-direction. Rather than generating energy travelling in only the positive x direction as we have assumed, a source at $x = 0$ would create waves traveling in both directions.

Verifying u(x,t) is a solution of the 1-D wave equation

Consider g$(t-x/v)$ and write $\eta = t - x/v$. Then, from the chain rule for partial differentiation

$$\frac{\partial g}{\partial x} = \frac{dg}{d\eta}\frac{\partial \eta}{\partial x} = -\frac{1}{v}\frac{dg}{d\eta} \quad \Rightarrow \quad \frac{\partial^2 g}{\partial x^2} = \frac{1}{v^2}\frac{d^2 g}{d\eta^2}$$

and $\quad \frac{\partial g}{\partial t} = \frac{dg}{d\eta} \quad \Rightarrow \quad \frac{\partial^2 g}{\partial t^2} = \frac{d^2 g}{d\eta^2}$

thus $\quad \frac{\partial^2 g}{\partial x^2} = \frac{1}{v^2}\frac{\partial^2 g}{\partial t^2}$, the 1-D wave equation

Similarly we can verify that $h(t+x/v)$ is a solution.

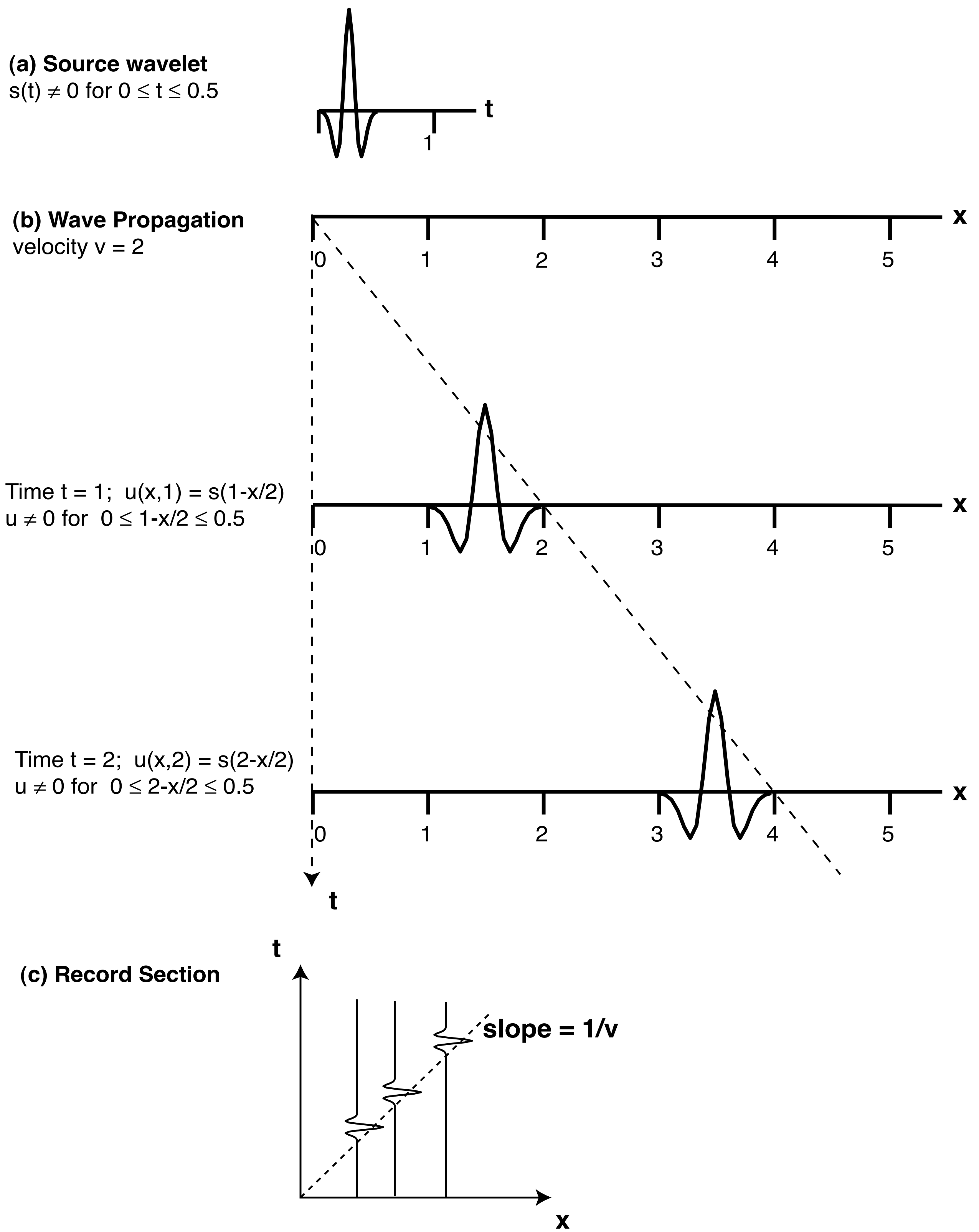

Figure 6 1-D wave propagation. A wavelet, *s(t)*, with a duration of 0.5 s created by a source at $x = 0$, (a), propagates without change in shape or amplitude with velocity, $v = 2\ km/s$ in the positive x-direction (b). If we create a record section from the seismograms of displacements recorded at a selected set of positions then the slope of the arrivals is equal to $1/v$ or 1/2.

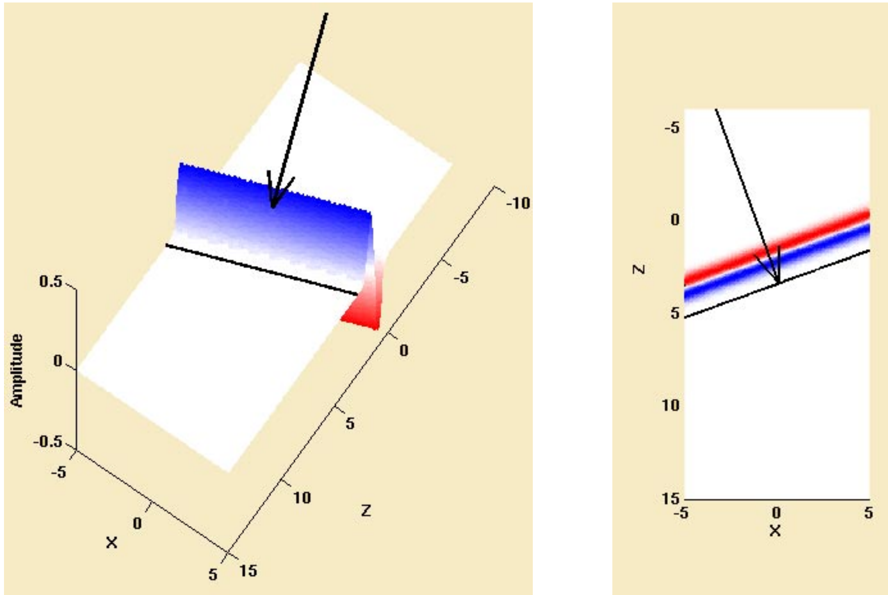

Figure 7: Perspective view and plan view of plane wave propagation in 2-D

2-D plane wave solution

If we assume that displacements in a solid are independent of y, then a particular solution, $u(\boldsymbol{x},t)$, of the 3-D scalar wave equation $\mathbf{n} = v\nabla T(\mathbf{x}) = \nabla r = e_r$

$$\nabla^2 u = \frac{1}{v^2}\frac{\partial^2 u}{\partial t^2} \qquad \text{(2 again)}$$

is given by $$u(\boldsymbol{x},t) = s(t - \frac{\sin\theta}{v}x - \frac{\cos\theta}{v}z) \qquad (5)$$

or equivalently by $$u(\boldsymbol{x},t) = s(t - px - qz) \;\; \text{where} \;\; \boldsymbol{p} = (p,q) = (\frac{\sin\theta}{v}, \frac{\cos\theta}{v})$$

As before, we can verify (5) is a solution of the wave equation by direct substitution in (2). Also if, as before, $s(t)$ represents a source wavelet that is non-zero for $0 \le t \le t_w$, then equation for the arrival time of the wave is found by setting the argument in (5) equal to zero (*c.f.* (4))

$$t - \frac{\sin\theta}{v}x - \frac{\cos\theta}{v}z = 0 \quad \text{or} \quad z = \frac{vt}{\cos\theta} - \tan\theta x \qquad (6)$$

This is the equation of a straight line or of a plane if one takes into account the *y* direction. From the analysis of the 1-D case, it can be seen that wave is propagating in the positive *x* and positive *z* directions. If, as is conventional in seismology, *z* is taken as the depth axis, then this is a wave propagating downwards into the earth at an angle θ to the horizontal. Equation (6) defines the leading edge of the wave, and is thus the equation of the *wavefront*.

Rays are defined to be everywhere perpendicular to wavefronts (strictly true only for isotropic media). The local ray direction can thus be found from the gradient of the wavefront equation (6).

Rewriting (6) as $t - T(\boldsymbol{x}) = 0$ where $T(\boldsymbol{x}) = \frac{\sin\theta}{v}x - \frac{\cos\theta}{v}z$

the ray direction, $\boldsymbol{n}$, satisfies $\boldsymbol{n} = v\nabla T(\boldsymbol{x}) = (\sin\theta, \cos\theta)$

In this case, the ray direction is constant and is at an angle θ to the vertical. The ray path, which is a line everywhere tangential to the ray direction, is a straight line. A ray path can be thought of as tracing the path taken by a small packet of energy centered on the ray (as a function of time).

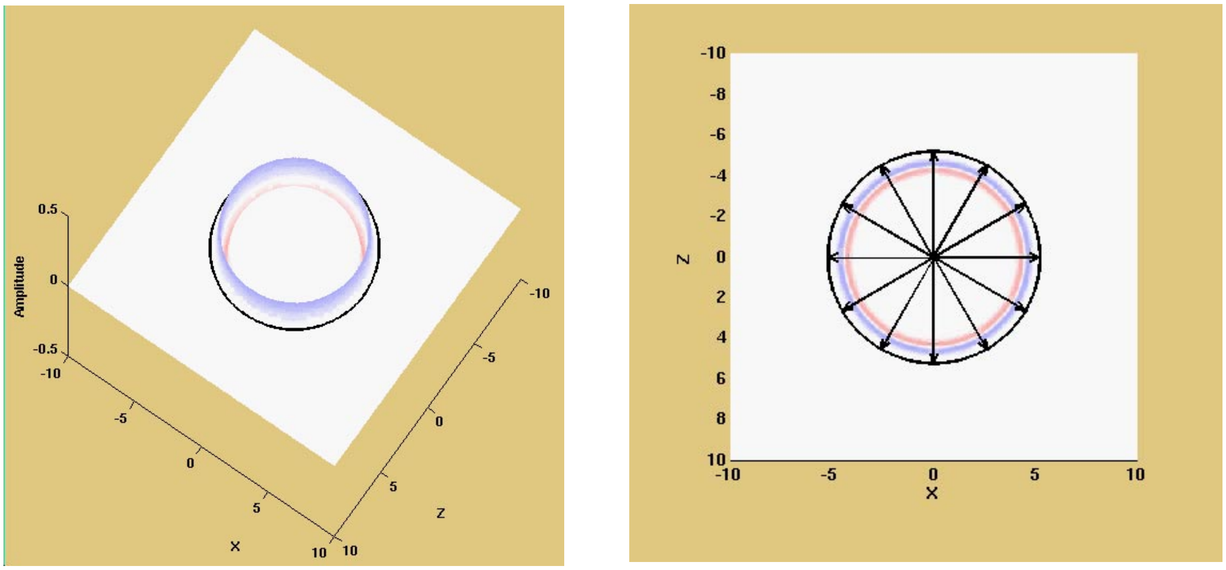

Figure 8: Perspective and plan view of a 2-D wave from a point source.

Point Source Solution

Another analytic solution of interest, is that for a point source. The solution, which by symmetry is a function only of radial distance r from the source and time, is derived in the accompanying text box and illustrated in Figure 8.

$$u(r,t) = \frac{s(t - r/v)}{r} \qquad (7)$$

Wavefronts & Rays:

As before we can find the wavefront by setting the argument of s equal to 0, that is

$$t - r/v = 0 \text{ or } \quad r = vt$$

The wavefront is spheres centered on the origin which expands with velocity v. The ray directions can be found as before from the gradient of $T(\mathbf{x}) = r/v$

$\mathbf{n} = v\nabla T(\mathbf{x}) = \nabla r = e_r$ where $\boldsymbol{e}_r$ is the unit radial direction.

The ray paths are radials with $r = vt\boldsymbol{e}_r$.

Geometric Spreading

The 1/r amplitude decay in (7) is said to be due to the geometric spreading of the wave. The source energy, E, is conserved just as in the previous cases but now the energy is spread out over progressively larger volumes. At time t, all the energy radiated away from the source is contained within a spherical shell of volume

$4\pi r^2 v t_w$ where t_w is the source duration

Assuming the energy is uniformly distributed, the energy density, E_ρ is

$$E_\rho = \frac{E}{4\pi r^2 v t_w}$$

Averaged over time, the energy is partitioned equally between kinetic energy and the potential energy of deformation. The potential energy is proportional to the maximum displacement amplitude squared (just as it is, for example, for a weight on a spring). Thus if the energy density falls of as r^{-2} then the amplitude of the seismic waves should decay as r^{-1}.

We can take r^{-1} as a representative amplitude decay rate for body waves. In the case of surface waves, the energy is trapped above a fixed depth, and for a point source the energy will be distributed over a cylindrical shell. Repeating the previous argument suggests that for surface waves a representative amplitude decay rate is $r^{-1/2}$. Thus at moderate distances from the source we can expect the amplitude of surface waves to be much larger than those of body waves.

General representation of body wave arrivals

We can rewrite our expression for a point source solution (7) to explicitly allow for the amplitude of the source –

$$u = A_o/r\ s(t-r/v)$$

Here we adopt the convention that the maximum displacement of s(t) is 1, so that A_o represents the amplitude of our seismic wave 1m from the source, this is usually be referred to simply as the source amplitude. At greater distance the amplitude is $A(\mathbf{x}) = A_o/r$, with the amplitude decaying due to geometric spreading.

Spherically symmetric solution for a point source

Assuming that spatial dependence of displacement for a point source is spherically symmetric, we need only consider r dependence for displacement, *u(r,t)*, and need only the radial part of the 3-D wave equation (2).

$$\frac{1}{r^2}\frac{\partial}{\partial r}\left(r^2\frac{\partial u}{\partial r}\right) = \frac{1}{v^2}\frac{\partial^2 u}{\partial t^2}$$

Expanding and rearranging

$$\frac{2}{r}\frac{\partial u}{\partial r} + \frac{\partial^2 u}{\partial r^2} = \frac{1}{v^2}\frac{\partial^2 u}{\partial t^2}$$

$$\frac{\partial^2 (ru)}{\partial r^2} = \frac{1}{v^2}\frac{\partial^2 (ru)}{\partial t^2}$$

\

This is the one-dimensional wave equation again only for *ru*. The general solution is thus

$$u(r,t) = \frac{g(t - r/v)}{r} + \frac{h(t + r/v)}{r}$$

Only the first part of the solution, propagating away from the source is physically appropriate thus

$$u(r,t) = \frac{g(t - r/v)}{r}$$

The solution apparently blows up at $r = 0$. In fact, any physical source will not be a point but will have a small but finite radius and we can think this solution as being valid beyond this radius.

We can generalize the form of the point source solution to produce a useful representation of a body wave arrival –

$$u(\mathbf{x},t) = A(\mathbf{x})\, s^{\dagger}(t-T(\mathbf{x})) \qquad (8)$$

where $A(\mathbf{x})$ represents the amplitude and the symbol $s^{\dagger}(t)$ allows for the fact that our source function might change shape during wave propagation. If the origin time of the source is t = 0, then wavefronts are, as before, given by

$$t = T(\mathbf{x})$$

and the ray directions by $\mathbf{n} = v\nabla T(\mathbf{x})$

Time Symmetry of the Wave Equation

The wave equation is unchanged if we reverse the direction of time, making the substitution $t' = -t$, leaves the form the 1-D wave equation unchanged

$$\frac{\partial^2 u}{\partial x^2} = \frac{1}{v^2}\frac{\partial^2 u}{\partial t'^2}$$

So are the solutions to the wave equation. For example, the general solution (3) of the 1-D wave equation is also unaltered in form but the direction of propagation is reversed

$$u(x,t) = g(-(t+x/v)) + h(-(t - x/v))$$

This observation is central to many of processes involved in seismic imaging of structure from seismic data, since it tells us that if we can develop a method to handle the forward problem of wave propagation we also have a tool for the inverse problem of imaging structure from our recorded energy.

Wavefronts and Rays

In the previous section, we looked at some simple analytic solutions to the wave equation and found the corresponding wavefronts and rays. There are only a limited number of such analytic solutions and to study more general cases we will concentrate on wavefronts and ray paths. These can be found using a pair of principles: *Huygen's principle* and *Fermat's principle*. In particular, we will use these principles to derive Snell's law for reflection and refraction at an interface. For the most part the earth models under consideration in later sections will consist of uniform velocity layers separated by interfaces for which Snell's law will be key.

Huygen's Principle

Huygen's principles states that successive positions of a wave can be found by assuming that all points on a wavefront at time t act as sources of secondary waves. The primary wave at time $t+\Delta t$ is the sum of the secondary waves. If the velocity near the origin of the secondary wave is constant, then the wavefront at time $t+\Delta t$ while be a circle of radius $v\Delta t$. If we looked at these secondary waves in detail we would find they have a complex radiation pattern; the amplitude would, for example, vary with direction. It is this complexity of amplitude and also of phase that allows the secondary waves to cancel exactly and reproduce the primary wave. If, however, we concentrate only on the wavefronts, there is no cancellation per se, but the primary wavefront at $t+\Delta t$ is the envelope of the secondary wavefronts, i.e. the surface that is tangent to the secondary wavefronts (See Figure 9a). The local ray direction is from the secondary source to the point of tangency of the primary and secondary wavefronts.
Since we using are wavefront-based/graphical interpretation of Huygen's principle, we need a few

rules to apply it successfully to more general situations:

(i) *There are 2 tangent surfaces for each set of secondary wavefronts*. This ambiguity is a consequence of the time symmetry of the wave equation. The same construction that finds the primary wavefront at time $t+\Delta t$ also finds it at $t-\Delta t$ (Figure 9b). External knowledge of the propagation direction to pick the appropriate envelope.

(ii) *Multiple origin times for secondary wavefronts*. The statement of Huygen's principal given above is in terms secondary sources originating at a fixed time. However, if we think of each point on the wavefront as a separate packet of energy traveling along its own ray path, then we can initiate secondary sources at times of our choosing. For example if we have secondary sources at times, t_1, t_2, t_3 *etc*. and we wish to find the primary at wavefront at t_c, the secondary wavefronts, in a uniform velocity medium would have radii $v(t_c-t_1)$, $v(t_c-t_2)$ *etc*. (see Figure 10).

(iii) *Reflections and diffractions*. In general, the secondary waves cancel out where they are not tangent to the envelope. The exception to this is if the origin of the secondary wavefront coincides with an abrupt change in material properties, If this change is continuous then the secondary energy sums up to produces a reflection in addition to the transmitted wave. If the change occurs within a small volume, effectively a point, the secondary does not cancel at all and we get a new wavefront originating at the point, a *point diffraction*.

(iv) A wavefront should not simply terminate at some finite point. It must either terminate either at a junction with some other part of the wavefront or possibly at infinity (see below). If a wavefront simply terminates at some point there is a flaw in the reasoning, often the cause is a forgotten point diffraction.

Fermat's Principle

Ray paths can be also found directly using Fermat's principle states that the ray path between any two fixed points is the path for which the travel time is a minimum (strictly the travel time need only be an extremum either maximum or minimum). For a uniform medium, the application of Fermat's principle shows, for example, that the ray paths are straight lines, since it is then equivalent to the statement that the shortest distance between two points is a straight line. From Fermat's principle one can also derive the *ray equations* which are a set of differential equations that can be integrated directly to find ray paths.

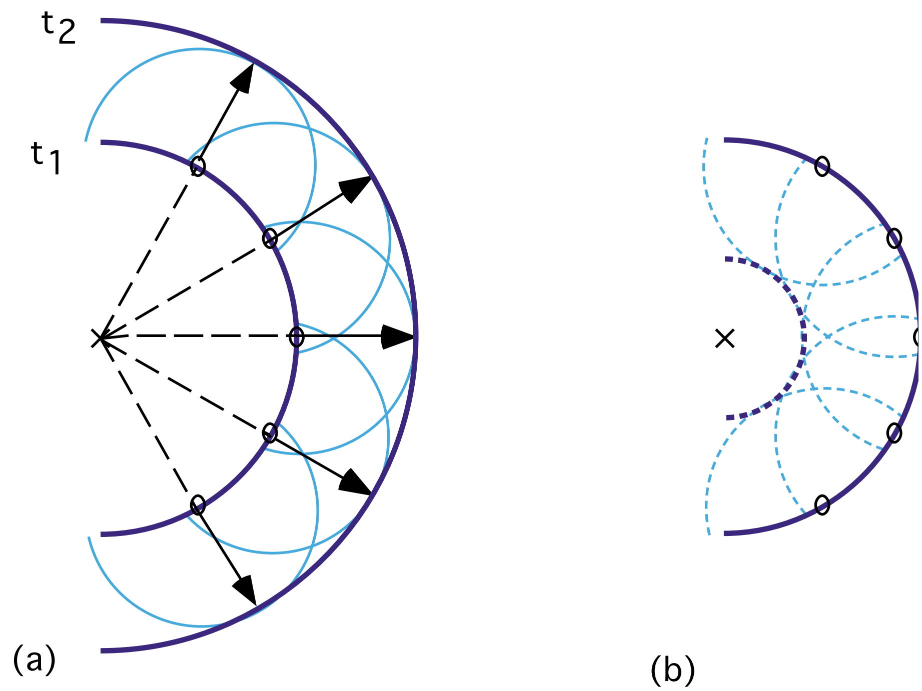

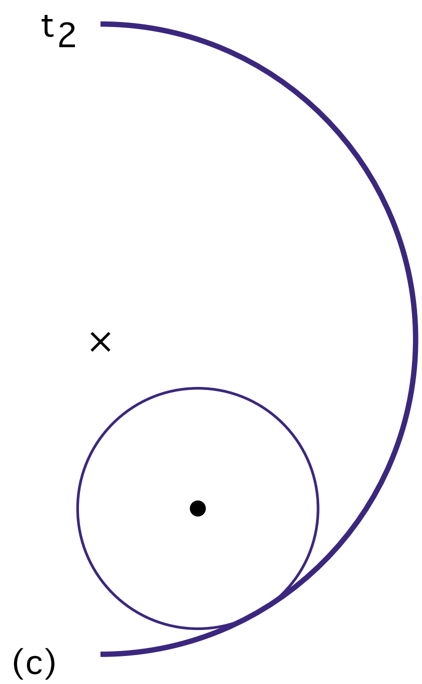

Figure 9 Huygen's Principle:

(a) A wavefront from a point source is expanding at a uniform medium of velocity v. We can construct the wavefront t_2 at time from the wavefront at time t_1 using Huygen's principle. The wavefront at time t_1 is taken as the being composed of secondary point sources. Each of these sources will produce a wavefront of radius $v(t_2 - t_1)$ at time t_2. The wavefronts of six secondary sources (cyan) are shown for source points indicated by small black circles. The primary wavefront at t_2 is the envelope of all these secondary wavefronts. The ray directions join the secondary source points to tangency of primary and secondary wavefront.

(b) The same construction can be used to determine the location of a wavefront at earlier times; a consequence of the time reversibility of the wave equation. The secondary wavefronts used in (a) will form a second envelope corresponding to the time $t_1 - (t_2 - t_1)$. (we have to supply external knowledge to decide which the actual direction of propagation.

(c) If there is an inhomogeneity in the medium, represented by the '•' , the secondary wavefront for this point will not cancel and will produce a point diffraction.

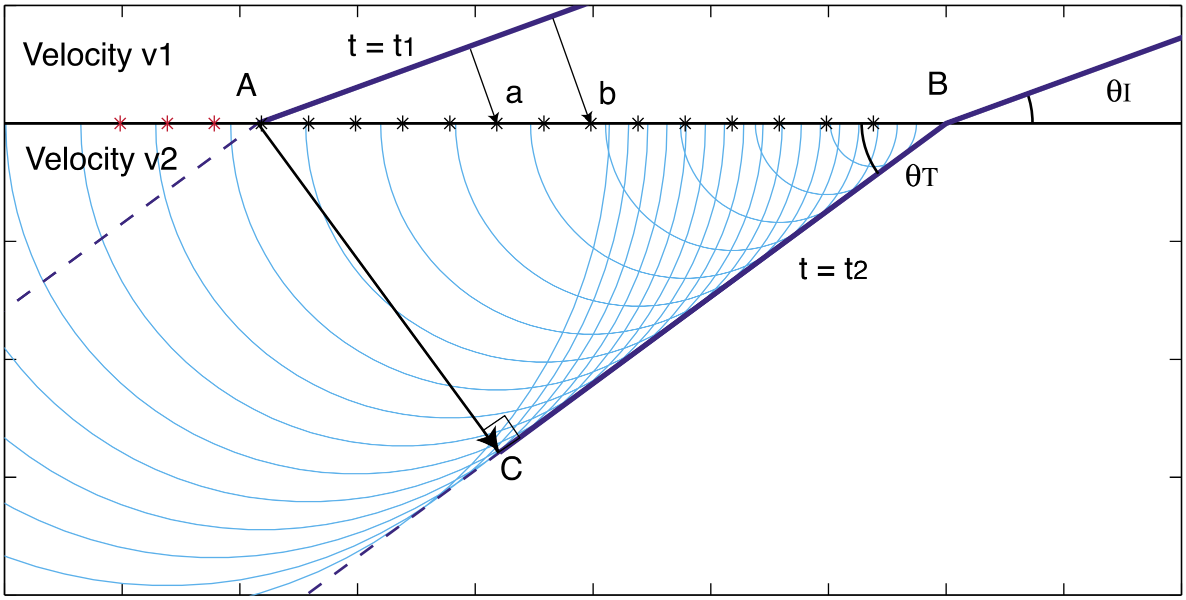

Figure 10a Plane wave refraction at an interface using Huygen's principle.

Application of Huygen's Principle to the Derivation of Snell's Law

A plane wave is propagating at an angle θ_I to an interface. The velocities of the two media are v_1 and v_2. Between times t_1 and t_2, the point of wavefront contact at the interface moves from A to B with an apparent velocity $v_{appr} = v_1/sin\theta_I$. As each point on the incident wavefront reaches the interface, e.g. a,b, it is treated as a source of secondary wavefronts in the lower medium. If we take the origin of the x-axis to be at A, the origin times for the secondary sources will be given by

$$t_o = t_1+x/v_{appr}$$

The radii of the secondary sources at time t_2 will be given by

$$r = v_2(t_2- t_0) = v_2(t_2-(t_1+x/v_{appr}))$$

Secondary wavefronts are shown in cyan. The envelope of the secondary wavefronts between A & B is the straight line BC, which is the refracted wavefront. Adding the results of secondary sources to the left of A (red *) extends the wavefront beyond C. N.B. The refracted wavefront originates at the interface and moves along the interface at the same apparent velocity as the incident wavefront.

The angle of refraction θ_T can be found from the fact that *AC* is a radius of the secondary wavefront and is perpendicular to *BC*. Triangle *ABC* is a right angle triangle and thus

$$sin\theta_T = AC/AB = v_2(t_2-t_1) / (t_2-t_1)v_1/sin\theta_I.$$

Rearranging yields $$sin\theta_I/v_1=sin\theta_T/v_2$$

This is a statement of *Snell's Law* applied to refraction at an interface.

We can go through essentially the same reasoning for reflection, Figure 10b. The origin times for the secondary sources are still

$$t_o = t_1+x/v_{appr}$$

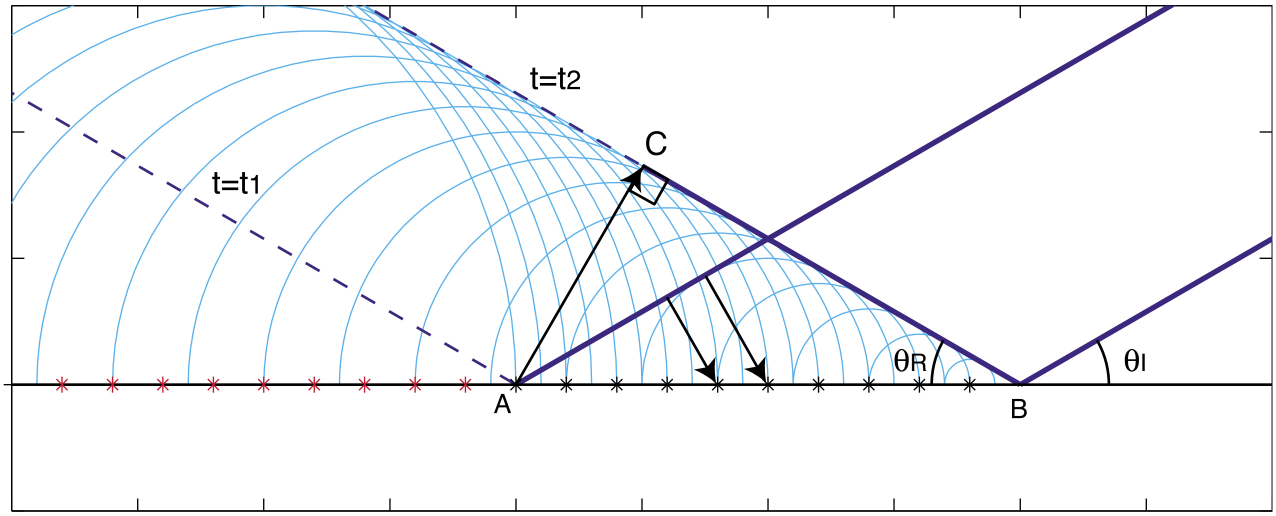

Figure 10b. Plane wave reflection at an interface.

Only now the radii of the secondary sources in the first medium are

$$r = v_1(t_2- t_0) = v_1(t_2-(t_1+x/v_{appr}))$$

Thus the angle of reflection θ_R is given by

$$sin\theta_I/v_1 = sin\theta_R/v_1$$

So the angle of reflection equals the angle of incidence, which is *Snell's Law* for reflection. Note again that the origin of the reflected wave is moving along the interface with the same apparent velocity, v_{appr}, as is the incident wave.

Application of Huygen's Principle to Complex Media

Figure 11 shows the results of a computationally efficient implementation of Huygen's method (*Rawlinson & Sambridge, Geophysical Journal International,* ***156****, 631-647, 2004*) used in a complicated medium with large continuous variations in velocity plus an interface. The source point is at the surface and marked by a star. The wavefronts, thin black lines, expand out from this point down towards the interface, thick black line. The wavefront becomes distorted to because the energy travels faster in the faster velocity material.

To calculate the reflection, the arrival times of the incident wavefront at the interface are recorded and used as the origin of secondary source reradiating energy back into the upper layer. The ray paths are found afterwards by connecting ray directions from wavefront to wavefront.

Fermat's Principle

Ray paths can be also found directly using Fermat's principle states that the ray path between any two fixed points is the path for which the travel time is a minimum (strictly the travel time need only be an extremum either maximum or minimum). For a uniform medium, the application of Fermat's principle shows, for example, that the ray paths are straight lines, since it is then equivalent to the statement that the shortest distance between two points is a straight line. From Fermat's principle one can also derive the *ray equations* which are a set of differential equations that can be integrated directly to find ray paths.

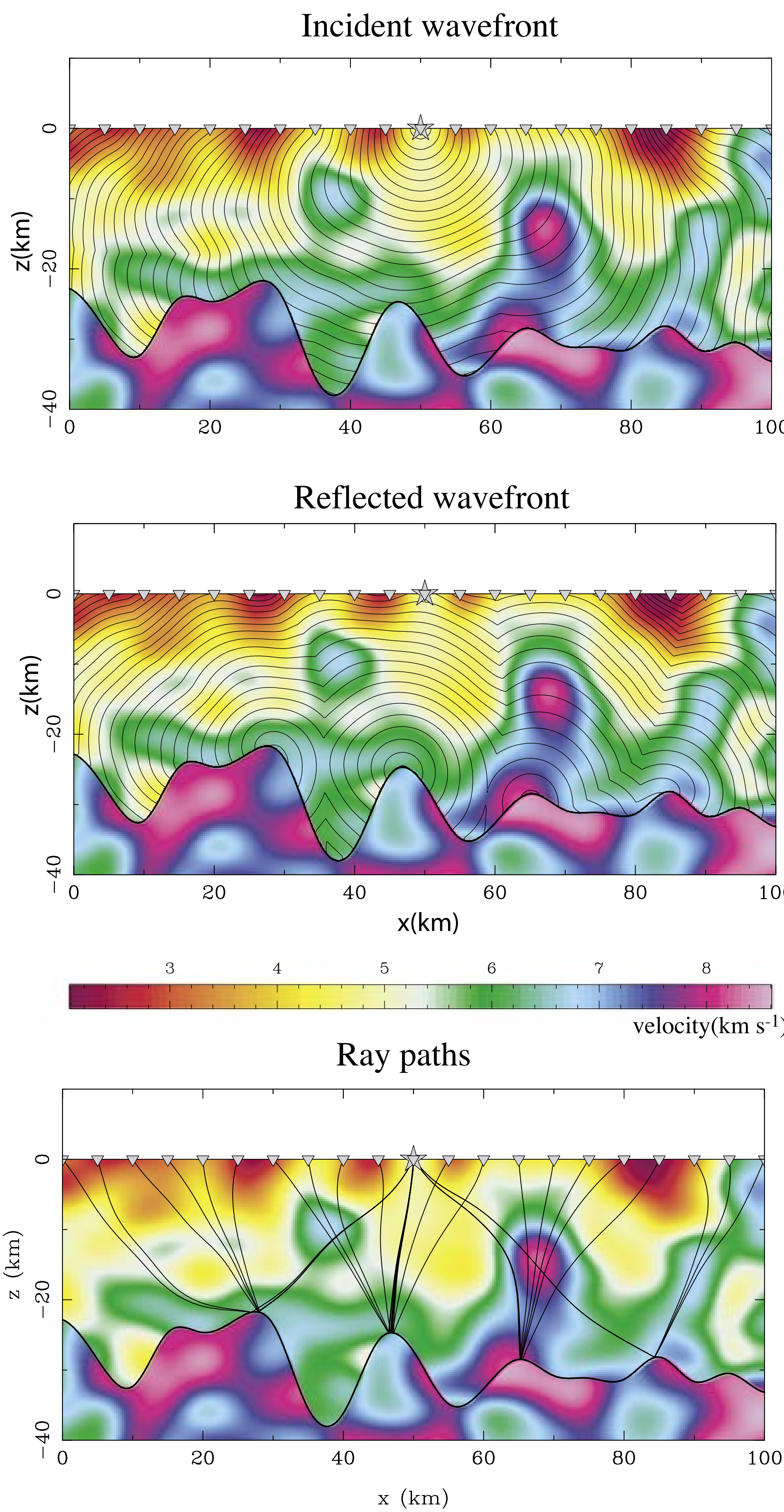

Figure 11 Calculation of wavefronts and ray paths in a layer with complex velocities.

Reflection and Refraction of a Plane Wave at an Interface

Combining the two results from the previous section into a single Snell's Law for refraction and reflection yields:

$$\frac{\sin\theta_I}{v_1} = \frac{\sin\theta_R}{v_1} = \frac{\sin\theta_T}{v_2} = \frac{1}{v_{appr}} = p \qquad (9)$$

Where θ_I is the angle of incidence of the plane wave, θ_R the angle of reflection, θ_T the angle of transmission. v_{appr} is the apparent velocity along the interface and p is known as the Snell parameter or horizontal slowness. The same result could have been obtained from Fermat's principle using rays. This can be interpreted physically as saying that, since the reflected and refracted wavefronts originate at the point of intersection of the incident wave with the interface, they must all travel along the interface with the same apparent velocity v_{appr}. The apparent velocity varies between infinity when $\theta_1 = 0°$ and the wavefront is parallel to the interface, and v_{p1} when $\theta_1 = 90°$ and the incident wave is perpendicular to the interface.

With wavefronts, angles are measured with respect to the interface, but for rays they are measured with respect to the normal to the interface.

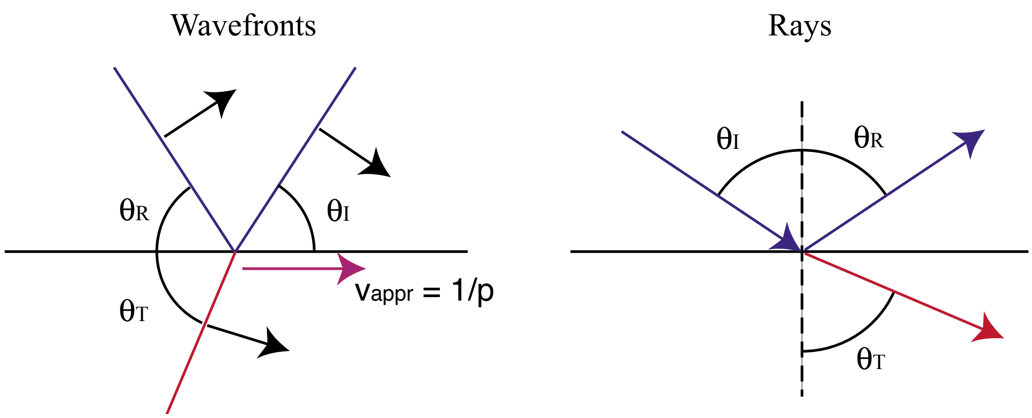

Figure 12: Angle definitions for a wavefront vs ray description. The wavefronts are drawn for some particular time, while the rays paths track the path time by some particular packet of energy.

For seismic waves life is a little more complicated because the solids on either side on an interface have both a P-wave velocity and an S-wave velocity. Thus for example an incident P-wave can give rise to a reflected S-wave in addition to a reflected P-wave, and a transmitted S-wave in addition to a transmitted P-wave. Snell's law for this case can be summarized succinctly by

$$\frac{\sin\theta_{PI}}{v_{p1}} = \frac{\sin\theta_{PR}}{v_{p1}} = \frac{\sin\theta_{PT}}{v_{p2}} = \frac{\sin\theta_{SR}}{v_{s1}} = \frac{\sin\theta_{ST}}{v_{s2}} = \frac{1}{v_{appr}} = p \qquad (10)$$

Subscripts P and S have been introduced to distinguish P and S waves.

When deriving Snell's law mathematically, one of the conditions that must be satisfied at the interface is continuity of displacement. For a P wave incident at any angle, particle motions are always confined to the vertical plane, as a consequence the particle motions of the reflected and transmitted waves are also constrained to the vertical plane, and the converted S-waves **must** be SV-waves.

Snell's law also applies in the case of an incident S-wave. In general, an incident S-wave will generate reflected and transmitted P-waves and S-waves. The angles are calculated using a modified version of equation (10) with the incident wave term replaced by $sin\theta_{s1}/v_{s1}$. However, if the incident S-wave is an SH wave with purely horizontal particle motions only reflected and transmitted SH waves are generated due to the requirement of displacement continuity. In this case, Snell's law simplifies back to equation

(9), providing the velocities are interpreted as S-wave velocities. In the case of a horizontally layered earth, wave motions thus decouple in a P-SV set and an SH set.

Critical Angles and Head Wave Generation

If $v_{p2} > v_{p1}$ then for an incident P-wave there is an angle, the *critical angle*, for which the angle of refraction for the P-wave is 90°, the wavefront is perpendicular to the interface and the refracted ray parallel to the interface. The value of the critical angle, θ_{pc}, is given by

$$\sin \theta_{PC} = \frac{v_{p1}}{v_{p2}} \tag{11}$$

At angles of incidence greater than P-wave critical angle, there is no transmitted P wave but there a transmitted S-wave. If the S-wave velocity in the second medium also satisfies $v_{s2} > v_{p1}$ then there will be a second critical angle beyond which there will be no transmitted S-wave either and all the incident energy will be reflected (total internal reflection).

A plane wave incident at the critical angle creates a transmitted/refracted wave that travels parallel to the interface in the faster medium. Conversely, a wave travelling parallel to the interface in the faster medium, creates a refracted waves or head waves in the slower medium which propagates away from the interface at the critical angle.

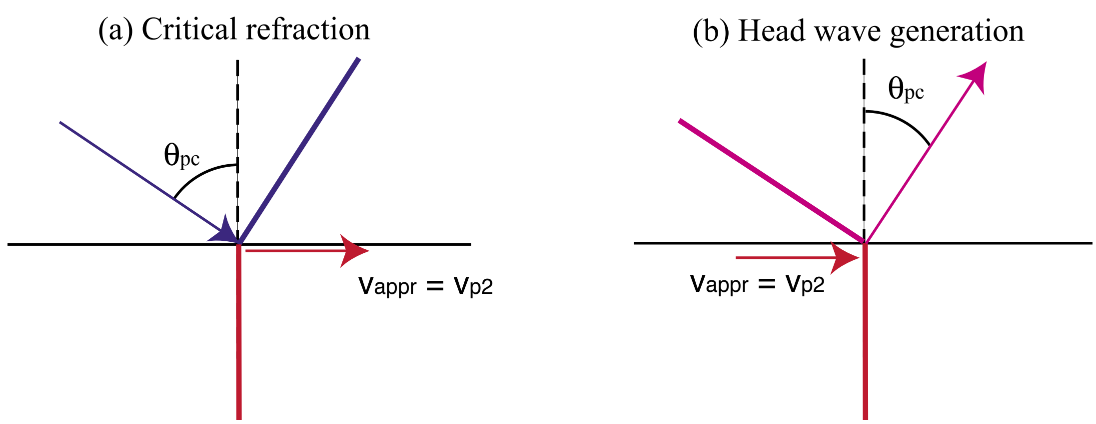

Figure 13 Critical refraction and head wave generation. (a) A wave incident at the critical angle is refracted so that wavefronts in the lower medium (red) are perpendicular to the interface. In terms of rays, the refracted ray is parallel to the interface. (b) Conversely, a wave travelling parallel to the interface in the lower medium generates a head wave (magenta) that propagates upwards at the critical angle in the first medium. For simplicity S-waves are ignored in this figure.

Generalization to non-planar cases

The above derivation of Snell's law relied on the fact that interface and wavefronts were planar. We can, however apply Snell's law to more complex wavefronts and interfaces by noting that both wavefronts and an interfaces are both locally planar if we look at a fine enough scale. (This is a high frequency approximation known as the *ray approximation*.). We apply Snell's law by find the normal direction to the interface at the point of intersection with the ray.

Layer over a Half-Space

The propagation of waves in a layer over a half-space from a surface point source can be analyzed using either wavefronts or rays. We will start by qualitatively considering the behavior of the wavefronts as a function of time. In the next section, we will develop a more quantitative ray description. In this discussion only P waves will be considered and thus we will drop the p subscript when referring to velocities and propagation angles.

For a layer over a half-space there are 3 parameters on interest; the thickness and velocity of the layer, denoted by h and v_1 respectively, and the velocity, v_2, of the half space below the interface. In the following example $h = 1$ km, v_1 = 1 km/s and v_2. = 1.5 km/s. The source point is at the surface at $x = 0$, and since the wavefield is symmetric about this point we only show $x > 0$.

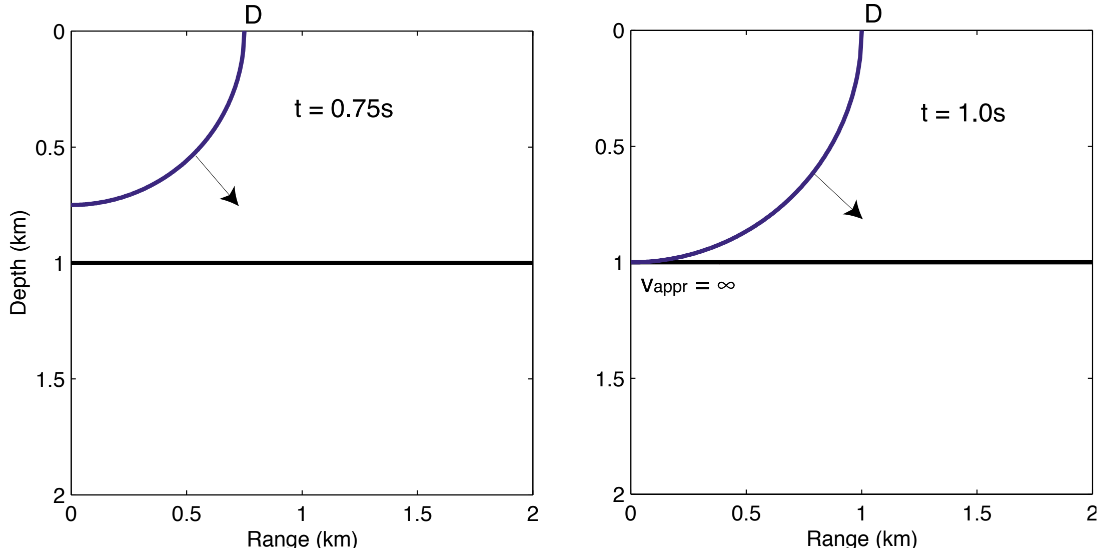

Figure 14a, initial expansion of the outgoing wavefront with the direct wave D traveling along the surface.

Before t = 1.0s, the outgoing wavefront is semicircular and hasn't reached the interface (Figure 14a). The only energy being recorded at the surface is the outgoing wavefront, D, which is the *direct wave* in the resulting seismic section.

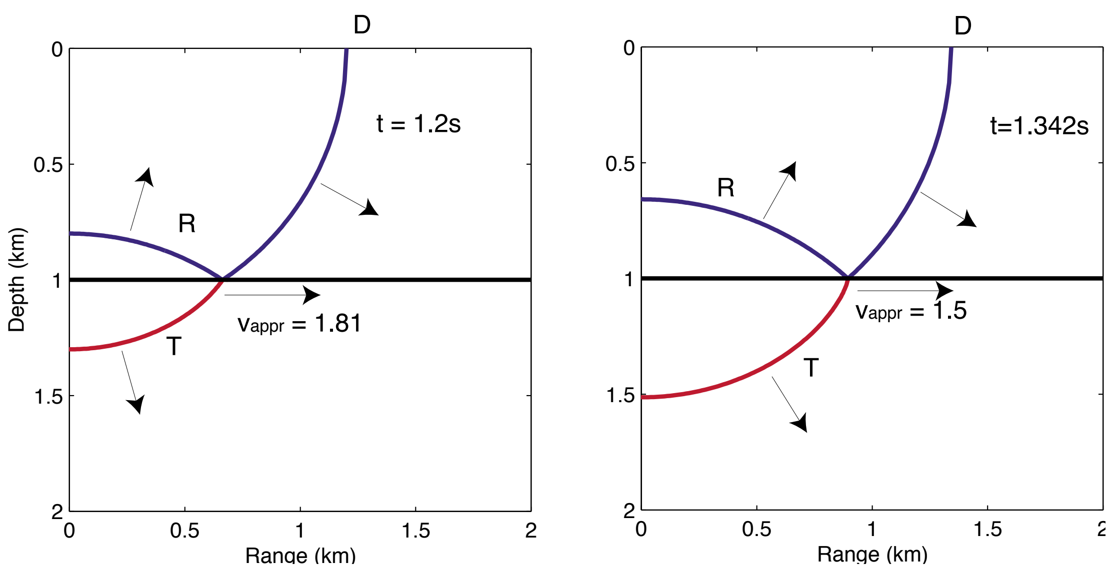

Figure 14b The incident wave starts to generate a reflected wave, R, and a transmitted wave T. v_{appr} is decreasing

After t=1.0 s, the incident wavefront at the interface starts to generate a reflected and transmitted wave, Figure 14b. The reflected wavefronts are circular arcs with an apparent source point at z = 2 km, the mirror image of the original source point in the interface.

Up until t = 1.342 s, the reflected, transmitted, and incident waves all meet on the interface. During this time the apparent velocity of the incident wavefront along the interface has slowed from infinite to v_2 (1.5 km/s). At this distance, the *critical distance* for the interface, the transmitted wavefront is perpendicular to the interface. The transmitted wave cannot slow down any further and from this point on will travel faster than, and separate from, the incident wave.

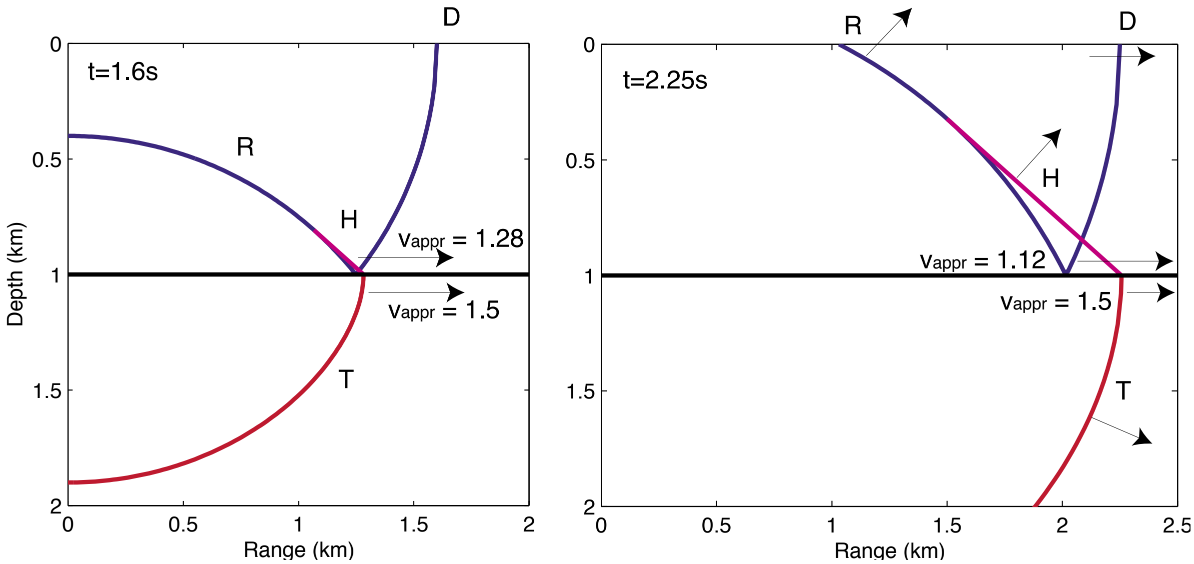

Figure 14c. After t =1.342s, the transmitted wave generates a head wave, H, (magenta) in the upper layer that propagates up towards the surface. After reaching the surface t=2.0s, the reflection appears as a recorded arrival at progressively greater ranges.

Once the transmitted wave begins outrunning the incident wave, it starts to generate a head wave, H, in the upper layer, Figure 14c. Since the apparent velocity of the transmitted wave along the interface is constant at 1.5 km/s, the head wave will be planar. The propagation angle of the head wave is, by Snell's law, equal to the critical angle, i.e. $\sin\theta_c = v_1/v_2$. Within the upper layer the head wave is tangential to the reflected wave (it cannot simply end at some arbitrary point).

At t=2.0s the reflected wave reaches the surface at x=0, and begins being recorded as it travels along the surface after the direct wave. At this time, reflected wave would start to generate a downward propagating *multiply reflected wave* but this is not shown.

When the head wave first arrives at the surface, it arrives with the reflection, (Figure 14d). This distance is referred as the *critical distance*. At greater distances, the head wave , which moves along the surface with an apparent velocity of v_2, will separate from the reflection and arrive earlier,. The head wave would itself reflect (not shown).

The direct wave travels along the surface with velocity v_1, always leading the reflected wave although by a constantly decreasing interval. In contrast, the head wave (refraction arrival) traveling at velocity v_2 will eventually overtake the direct wave at the *crossover distance*.

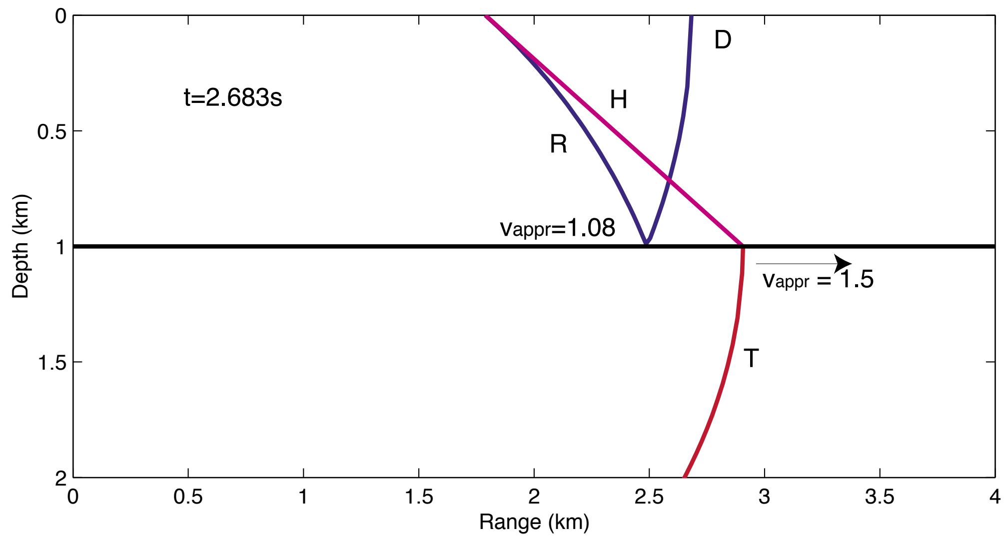

Figure 14d. At t=2.683s, the head wave first arrives at the surface with the reflection. This distance is known as the critical distance. The head wave is not seen at shorter distances.

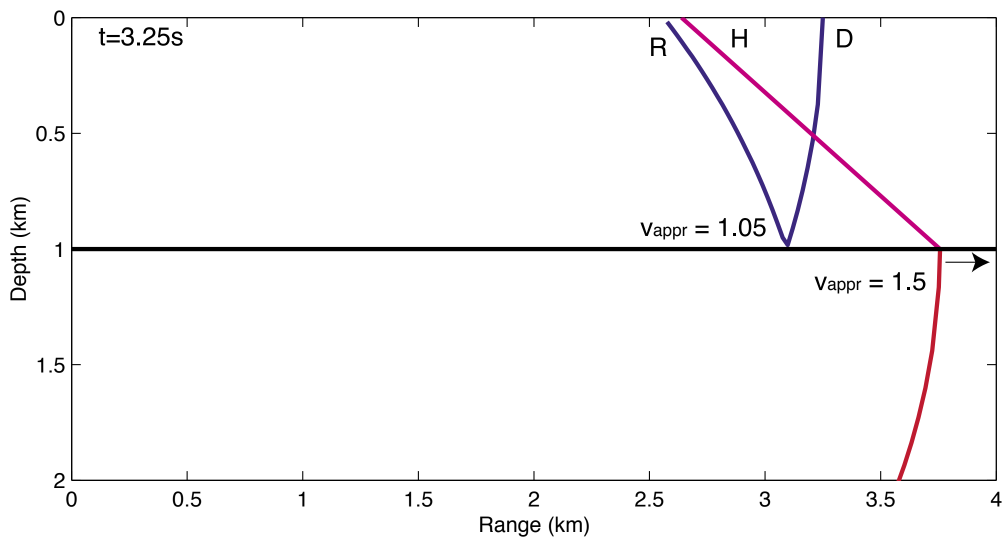

Figure 14e. For t > 2.683s the head wave arrives ahead of the reflected wave. Eventually it will overtake the direct wave as well and become the first arriving energy on the seismic section.

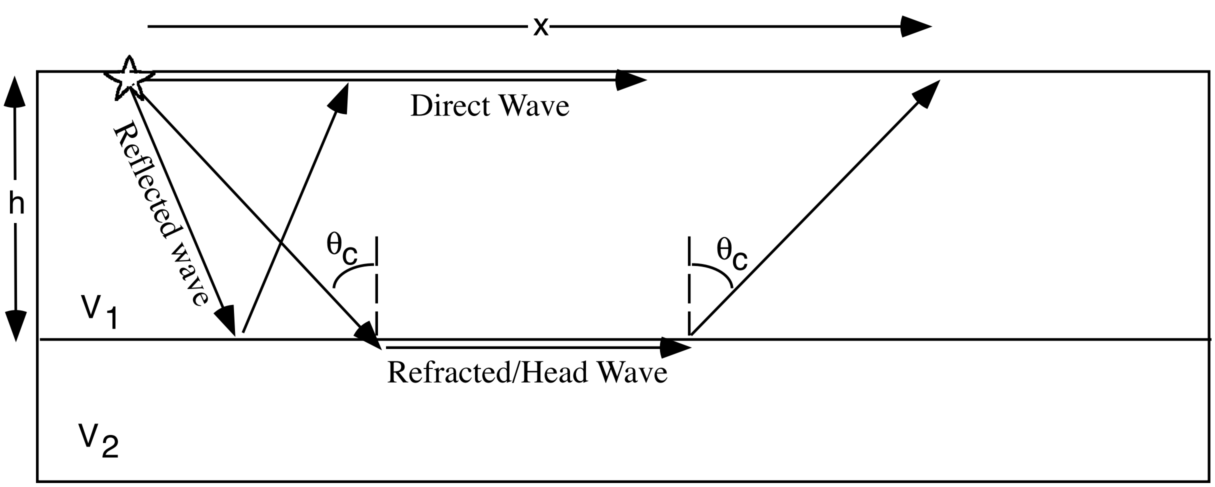

Figure 15 Ray paths for a layer over a half space. The rays paths for direct, reflected and refracted/head wave arrivals are shown. The propagation angle for the head wave in the top layer is the critical angle.

Travel Times & Distances

The travel times, t, for the three arrivals of interest, the direct wave, the reflection arrival, and the refraction arrival/head wave arrival can all be calculated as a function of source-receiver distance x by drawing ray paths and using elementary geometry.

Direct Wave

The direct wave simply travels along the surface, and it's travel time is:

$$t = \frac{x}{v_1} \tag{12}$$

Reflection

Since the downgoing and reflected ray paths are symmetric, the reflection time, t, can be found by applying Pythagoras's theorem to the downgoing part of the path and using half the source-receiver offset or rearranging

$$\left(\frac{v_1 t}{2}\right)^2 = \left(\frac{x}{2}\right)^2 + h^2$$

Denoting, the two-way reflection time at vertical incidence by t_o, i.e.

$$t_o = \frac{2h}{v_1} \tag{13}$$

The reflection time can be written as:-

$$t^2 = t_o^2 + \frac{x^2}{v_1^2} \tag{14}$$

Thus the path of the reflection in t-x space is a *hyperbola*. At large ranges, the reflection equation is approximated by $x = v_1 t$ and thus the reflection asymptotes to the direct wave.
x^2-t^2 method: The velocity of the layer can be estimated either from the curvature of the hyperbola or by plotting t^2 as a function x^2 and estimating the best fitting straight line. This method known, as the *x^2-t^2 method*. Once the velocity has been estimated from the slope of the line, the thickness of the layer can be estimated from the intercept, which is t_o^2 .

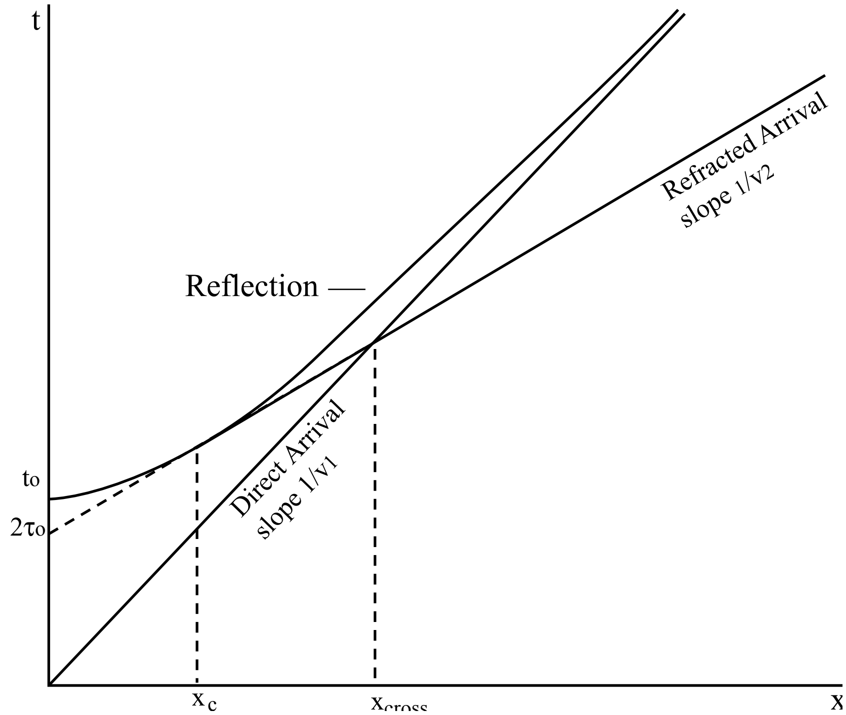

Figure 16 Travel time curve for layer over a half space. Curves are plotted as a function of source-receiver distance x. The refracted arrival separates from the reflection at the critical distance x_c. It becomes a first arrival beyond the crossover distance x_{cross}, where it intersects the direct arrival.

Refraction/Head Wave

For the refracted arrival, the angle of the downgoing and upgoing ray at the interface equals the critical angle, θ_c. The total travel-time is the sum of the equal down and up going ray paths plus the time spent traveling along the interface

$$t = \frac{2h}{v_1 \cos\theta_c} + \frac{(x - 2h\tan\theta_c)}{v_2}$$

$$t = \frac{2h}{v_1 \cos\theta_c}\left(1 - \frac{v_1}{v_2}\sin\theta_c\right) + \frac{x}{v_2}$$

Using the fact that the critical angle is given by $\sin\theta_c = \frac{v_1}{v_2}$,this simplifies to

$$t = \frac{2h\cos\theta_c}{v_1} + \frac{x}{v_2}$$

or writing τ_o for $\frac{h\cos\theta_c}{v_1}$

$$t = 2\tau_o + \frac{x}{v_2} \qquad (15)$$

$2\tau_o$ is known as the *intercept time* or *vertical delay time*. The travel-time curve for the refraction is a straight line, with a slope equal to the reciprocal of the half-space velocity. The velocity in the layer is derived from the slope of the direct wave, which obviously has the form of the refraction arrival but with zero intercept time. The depth of the layer, *h*, can be estimated from the delay time, to, once the two velocities have been found.

$$h = \frac{v_1\tau_o}{\cos\theta_c} \qquad (16)$$

Critical Distance

The critical distance, x_c is the distance at which the refraction separates from the reflection. It is the distance at which the ray reflected at the critical angle arrives back at the surface, since this ray can also be regarded as a refraction arrival that travels zero distance along the interface.

$$x_c = 2h\tan\theta_c = \frac{2hv_1}{v_2\cos\theta_c} = \frac{2hv_1}{\left(v_2^2 - v_1^2\right)^{\frac{1}{2}}} \tag{17}$$

Crossover Distance

The crossover distance is the distance at which the refraction crosses the direct arrival thus the refraction time (36) equals the direct-wave time (30)

$$\frac{x_{cross}}{v_1} = \frac{2h\cos\theta_c}{v_1} + \frac{x_{cross}}{v_2}$$

Rearranging and substituting for $cos\theta_c$

$$x_{cross}\left(1 - \frac{v_1}{v_2}\right) = 2h\left(1 - \frac{v_1^2}{v_2^2}\right)^{\frac{1}{2}}$$

simplifying

$$x_{cross} = 2h\left(\frac{v_2 + v_1}{v_2 - v_1}\right)^{\frac{1}{2}} \tag{18}$$

The crossover distance is at least twice the depth to the refractor. A rule of thumb is that the crossover distance is 3-5 times the depth of the refractor. For example in marine seismic work, the thickness of the oceanic crust is typically 6 km, the water depth is 3-4 km and the distance of the Moho refraction is around 30 km.

Data Examples

In the foregoing calculations we have ignored the S-waves, multiple reflections and surface waves that would be present in actual data. Multiple reflections are simply arrivals that have been reflected at multiple interfaces before reaching the receiver. A distinction is made between *internal multiples*, energy reflected multiple times in the subsurface, and *surface multiples* that include one reflection at the earth's surface. Surface multiples are particularly strong and readily identifiable in marine experiments with a hard seafloor. We illustrate the importance of surface waves and multiples in reality with a model dataset and a dataset collected with a hammer seismograph

Figure 17a shows a simple model of a sedimentary basin with five uniform velocity layers, and Figure 17b shows a computed record section for this model that includes all the body waves and internal multiples but ignores the surface. A *record section* is a collection of seismograms with a common property, in this case they are all records of vertical ground motion from a single seismic source. A record section with this property is also referred as a *shot gather.* In this shot gather there are 48 seismograms or *traces* (as they are often called) with source-receiver ranges, or *offsets,* evenly spaced at 50 m intervals between 0.1 & 2.45 km. The arrivals that we calculated for a layer over a half space are present - the direct wave, D, the reflection from the first interface, R1, and the head wave from the first interface, H1.

The arrivals R2-R5 are P-waves reflected from the deeper interfaces. Calculating their travel times as a function of offset (range), is more complicated than for the first interface, but it is simple to calculate the reflection times at *zero offset* or *vertical incidence,* where the appropriate ray paths are ones that

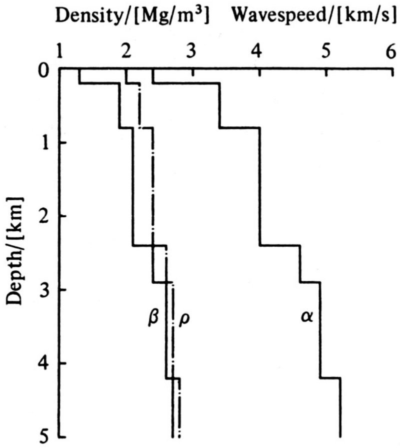

Depth (km)	V_p (km/s)	V_s (km/s)	Density (Mg/m^3)
0.0 - 0.2	2.4	1.3	2.0
0.2 - 0.8	3.4	1.9	2.2
0.8 - 2.4	4.0	2.1	2.4
2.4 - 2.9	4.6	2.4	2.6
2.9 - 4.2	4.9	2.6	2.7
4.2 -	5.2	2.6	2.8

Figure 17 a) A simplified, one-dimensional model of a sedimentary basin. The model consists of 5 uniform velocity layers separated by interfaces at which velocity increases.

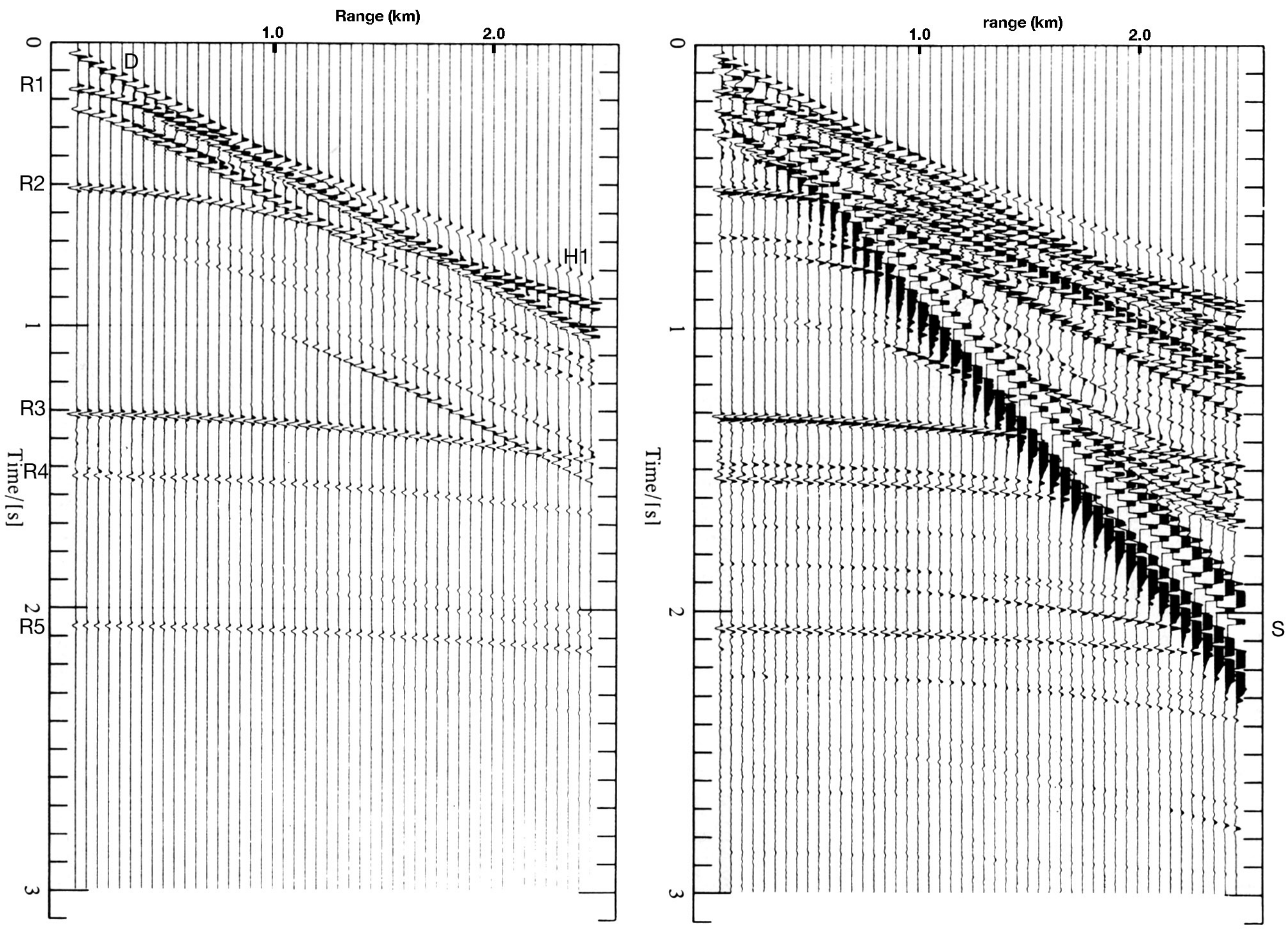

Figure 17 b) Primary reflections and internal multiples. Indicated are the direct wave, D, the head wave from the first interface, H1, and the primary P-wave reflections from the interfaces, R1 - R5. At further offsets P-S converted phases are evident. There are 48 traces with a minimum offset of 0.1 km, a maximum offset of 2.45 km and an trace spacing of 50 m. (c) Including free surface reflections. There is a now a high-amplitude Rayleigh wave train, S, multiples within the surface layer, that become particularly strong and complicated at larger offsets after the R1 reflection. The surface wave arrivals have been clipped during plotting.

travel vertically down to and up from the reflecting interface. The travel time contribution from each layer *i* is simply $t_i = 2h_i/v_i$, where h_i is the thickness of the i^{th} layer. The total reflection time is

$$t_n = \sum_{i=1}^{n} T_i = \sum_{i=1}^{n} \frac{2h_i}{v_i}$$

Thus, for example, the vertical incidence reflection time for R2 is

2*0.2/2.4 + 2*0.6/3.4 = 0.51 s,

and for R3 is 0.51+ 2*1.6/4 = 1.31 s.

In Figure 17c, the earth's surface was included in the calculation. There is now a high-amplitude, slow-moving fundamental Rayleigh wave, S, and surface multiples that create a complicated set of arrivals in a wedge between the first arriving refractions and the fundamental Rayleigh wave. The arrivals that are still relatively easy to identify are the first arriving refraction arrivals (and perhaps a closely following secondary reflection at further offsets), which is the data used for refraction seismology, and the reflection arrivals at small offsets, which is the data used for reflection seismology.

Hammer Seismograph Example

A real-world example of this complexity is shown in Figure 18, which is data from a small-scale seismic refraction experiment using a sledgehammer as the source, Figure 18. The objective of such an experiment can be to find the depth and shape of bedrock as part of a site survey for a construction project. If the depth to bedrock is only a few meters then a sledgehammer and muscle power produce sufficient source energy.

An inertial switch attached to the hammer closes when the hammer strikes the ground, initiating recording on the *seismograph*. The receiver array is a line of uniformly spaced *geophones*. The most commonly used geophones measure the vertical velocity of ground motion. Detectable ground motions typically have particle velocities on the order of 10^{-8} ms^{-1}, and corresponding ground displacements of 10^{-10} m. In contrast the velocity of seismic wave propagation is 10^2 - 10^3 m/s. In detail the seismograms are complex, but once again it is relatively easy to pick the time of the first arriving energy, the red line in Figure 19.

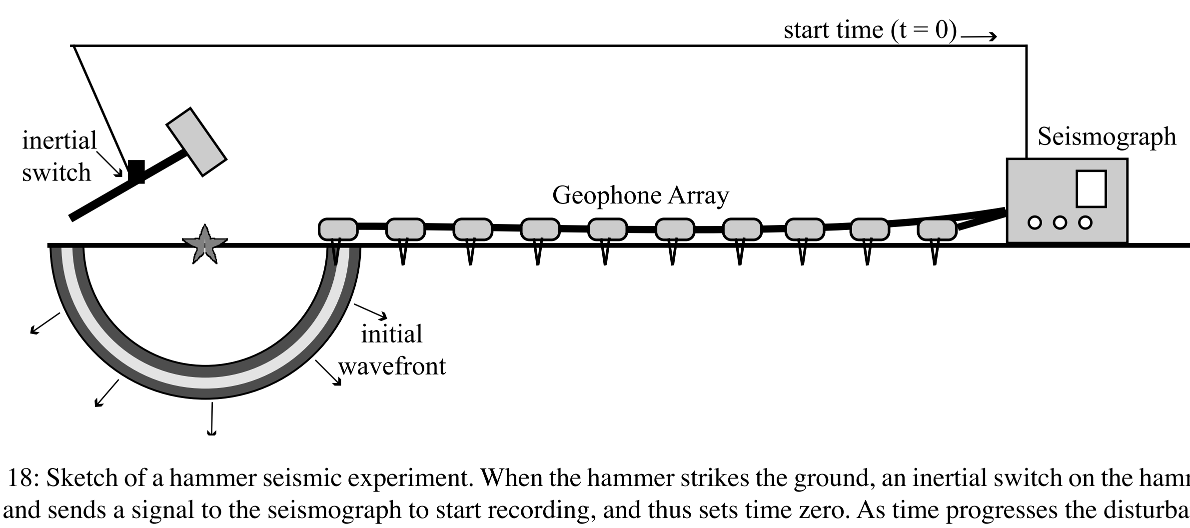

Figure 18: Sketch of a hammer seismic experiment. When the hammer strikes the ground, an inertial switch on the hammer closes and sends a signal to the seismograph to start recording, and thus sets time zero. As time progresses the disturbance caused by the hammer blow spreads out from the source point and is recorded by the geophone array. The initial wavefront, separating the undisturbed and disturbed material corresponds to the primary wave or P-wave. The details of the disturbance behind the P-wave are typically complex.

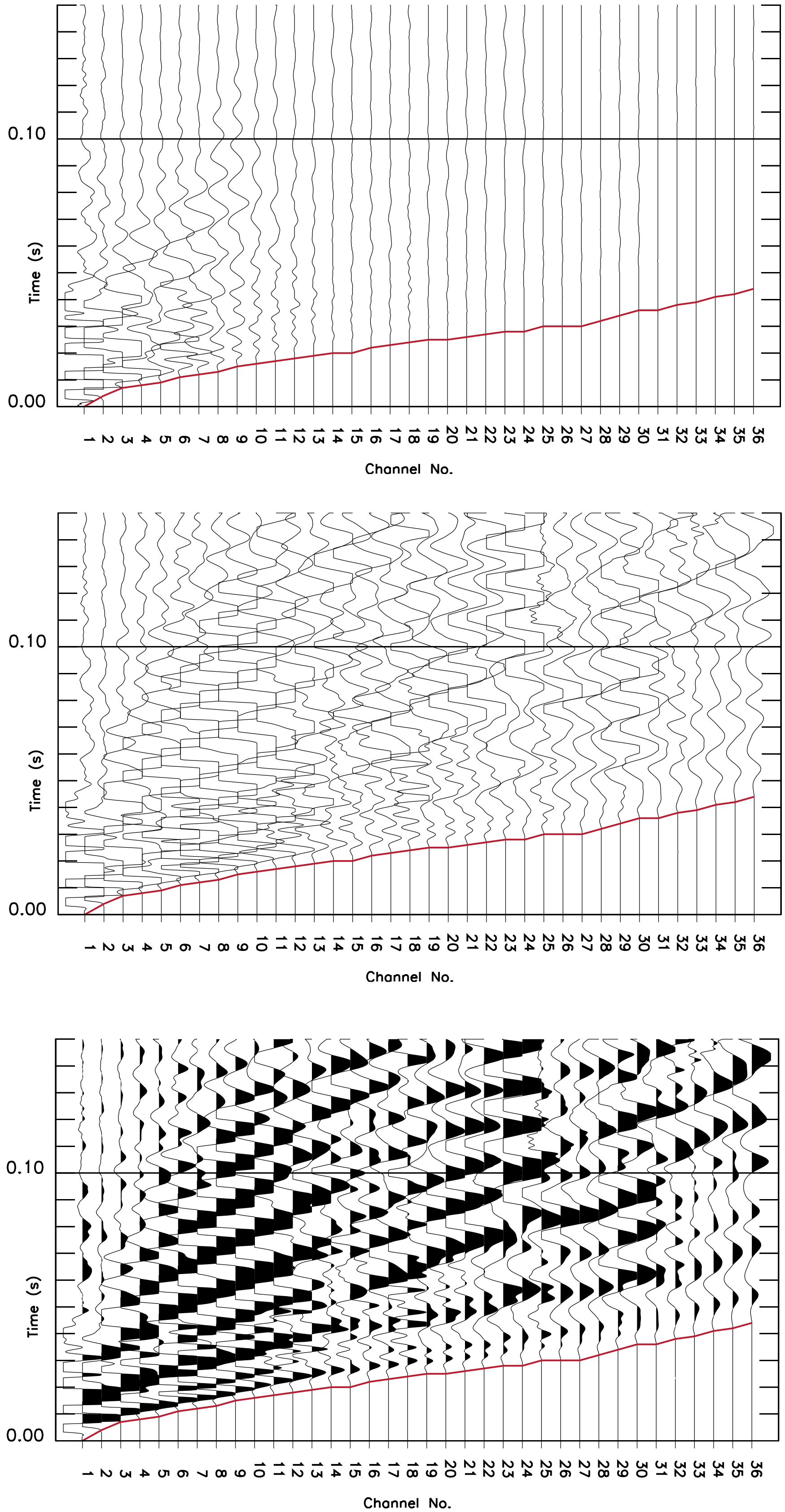

Figure 19: Example record section for a hammer seismic experiment. The output seismograms are labeled by the recording channel no. on the seismograph. Channel no. 1 corresponds to the output from a geophone 0.5 m from the source. The geophone spacing is 1.5 m, and the maximum offset is 53 m.

The different plots are different presentations of the same record section. The red line marks the arrival time of the P wave at the different geophones. In the top section, the data is plotted with a uniform gain, only arrivals at small offsets and early times are visible. In the middle section, amplitude corrections have been applied during plotting, making arrivals at latter times and larger ranges visible. In the bottom section the positive parts of the seismograms have been filled black, helping the eye correlate arrivals between seismograms.